National Centre for Energy and Environment,
Energy Commission of Nigeria, University of Benin:
ISSN 2504-9593
DOI: 10.5281/zenodo.18750071
https://ijree.com/index.php/publications/article/view/32
Int. J. Renew. Energ & Environ Vol.4 (1), pp 47-57(2026)

IMPROVED (SPER) DESIGN WITH SOLAR-DRIVEN AIRFLOW AND CONTROLLED WATER CIRCULATION FOR REDUCED POSTHARVEST LOSSES IN SEMI-ARID OFF-GRID SETTINGS

Musa, H[1].; Maina, M. B[1].; Muhammad, A. B[1]., Abdulrahim, A. T[2]., Abdulrahaman, S.A[1].
[1]Department of Mechanical Engineering, University of Maiduguri, Borno State, Nigeria
[2]Department of Mechanical Engineering, Kwara State University, Kwara State, Nigeria
Corresponding author: harunadabujii@gmail.com

Abstract

Off-grid communities in Borno State face persistent challenges in preserving perishable food commodities due to high ambient temperatures, low relative humidity, and unreliable electricity supply. These constraints result in significant postharvest losses, weaken local food security, and limit the economic viability of smallholder farmers and informal food vendors. Conventional refrigeration systems, particularly vapor-compression technologies, are largely unsuitable in such contexts because of their high energy demand, dependence on continuous grid power, and environmental concerns associated with synthetic refrigerants. This study examines the viability and performance potential of a Solar-Powered Evaporative Refrigerator (SPER) as a sustainable cooling solution for off-grid environments. Constructed primarily from locally available, low-cost materials, the system was designed for autonomous operation, environmental sustainability, and scalability. Field testing under representative semi-arid conditions (ambient temperatures of 32–41 °C and relative humidity of 18–35%) demonstrated a maximum internal temperature reduction of up to 12 °C, alongside increased internal relative humidity suitable for fresh produce storage. Performance evaluation showed that the SPER reduced tomato spoilage by approximately 75% over a 72-hour storage period, significantly outperforming conventional non-insulated Zeer pots. Thermal analysis revealed that the combined effects of clay-based insulation, sustained fibre saturation, and solar-driven airflow were critical in stabilizing internal temperature and humidity levels, while maintaining low water and energy consumption. Overall, the findings confirm the SPER's potential as a low-energy, decentralized refrigeration technology for resource-limited, off-grid settings. Its adaptability to tomatoes and other perishable commodities offers a practical pathway to reducing postharvest losses, improving food security, and promoting environmentally friendly cooling solutions in semi-arid regions.

Key words; Solar-powered, evaporative refrigeration, Semi-arid, postharvest storage, insulation, Low-energy

1. Introduction

Reliable refrigeration remains limited in many off-grid and energy-scarce communities, particularly in semi-arid environments such as Maiduguri, Nigeria. High ambient temperatures, unreliable electricity supply, and limited cold-chain infrastructure exacerbate postharvest losses and undermine food security Sibanda and Workneh (2020). While vapor-compression refrigeration dominates conventional cold storage, its application in off-grid contexts is constrained by high energy demand, dependence on continuous electricity supply, elevated lifecycle costs, and environmental concerns associated with HFC and HCFC refrigerants (Yahaya et al., 2018; Shailaja, 2018). Thermodynamic analysis in Nigeria highlights natural refrigerants (e.g., R-717/ammonia) in vapor compression systems, achieving superior COP under local high-ambient conditions (30-40°C), Oyedepo and

Adenle (2025). Evaporative cooling technologies, particularly solar-powered evaporative refrigerators (SPERs), have therefore emerged as promising low-energy alternatives for short-term food preservation in hot climates Bello and Musa (2025). Operating on latent heat absorption during water evaporation, SPER systems can achieve substantial temperature reductions without grid electricity. However, their performance is fundamentally constrained by psychrometric limits, with maximum cooling bounded by ambient wet-bulb temperature Djordjevic and Dincă (2025). Several studies report effective cooling primarily under low-to-moderate relative humidity conditions, typically below 35–40%, beyond which evaporative potential declines sharply (Prabodh, 2016; Baloch et al., 2018). Tests across four configurations (conventional, magnetized water, heat exchanger, combined) demonstrated up to 93.97% efficiency, limited by low evaporation rates and humidity control without material and exposure optimizations, Alshukri *et al*,. 2025, recent reviews argue that system design—particularly insulation quality, airflow management, and water delivery control—can significantly extend functional performance into moderately humid regimes (Xue et al., 2023; Abbas et al., 2025). This divergence highlights that climatic suitability alone does not fully determine evaporative cooling effectiveness; rather, thermal resistance, evaporative surface characteristics, and system control strategies play decisive roles. Conventional Zeer pot systems, though culturally embedded and low-cost, often suffer from inadequate thermal insulation, uncontrolled water evaporation, and large diurnal temperature fluctuations, limiting their practical scalability (Ronoh *et al.,* 2020). Empirical studies consistently show that uninsulated systems experience high conductive heat gains, reducing effective cooling even under favorable ambient conditions.

Recent research has therefore shifted toward hybridization and material optimization. Solar-assisted water circulation, desiccant preconditioning, and improved porous media have been shown to enhance evaporation efficiency and thermal stability (Mugwaneza et al., 2024). In parallel, the incorporation of agricultural waste fibers and porous additives into clay matrices improves water retention and evaporative surface area while reducing environmental impact (Ronoh et al., 2020; Haile et al., 2024). Emerging studies further demonstrate that IoT-enabled monitoring can mitigate performance variability by enabling adaptive water and airflow control (Abbas et al., 2025). Despite these advances, a critical gap remains: field-based, thermodynamically grounded comparisons between improved insulated SPER systems and conventional non-insulated Zeer pots under representative semi-arid conditions are scarce. Many studies either rely on laboratory testing or lack normalization against wet-bulb limits, limiting cross-study comparability and real-world relevance.

2. Materials and Methods

2.1. Materials and System Components

The solar-powered evaporative refrigerator (SPER) was fabricated using locally sourced terracotta clay for both the inner and outer storage chambers and natural jute fibre as the evaporative medium, consistent with established evaporative cooling studies (Prabodh, 2016; Yahaya et al., 2018). The energy subsystem consisted of a 50 W monocrystalline photovoltaic (PV) panel, a 10 A PWM charge controller**,** and a 12 V, 40 Ah deep-cycle lead–acid battery, providing autonomous off-grid operation. Air circulation was achieved using a 12 V DC axial fan with a nominal airflow rate of 85 m^3 h^{-1}**,** while water distribution across the jute fibre was maintained by a 12 V submersible DC pump delivering 0.5 L min^{-1} at a head of 1.2 m. These values were selected to balance evaporative effectiveness with low electrical power demand.

Environmental parameters were monitored using calibrated instruments: digital thermometers (±0.5 °C) for internal and ambient temperatures, digital hygrometers (±2% RH) for relative humidity, and a hot-wire anemometer (±0.1 m s^{-1}) for airflow verification. Water consumption was measured using a graduated cylinder (±10 mL), while material mass changes were determined with an electronic weighing balance (±1 g). The materials, equipment and key system specifications are given in table 1.

Table 1. Materials, equipment, and key system specifications

Component	Specification
PV panel	50 W, 12 V monocrystalline
Battery	12 V, 40 Ah deep-cycle
Charge controller	10 A PWM
DC axial fan	12 V, 85 $m^3 h^{-1}$ airflow
Water pump	12 V DC, 0.5 L min^{-1}
Clay pots	Inner wall ≈10 mm; outer wall ≈20 mm
Evaporative medium	Natural jute fibre
Temperature sensor	±0.5 °C accuracy
Humidity sensor	±2% RH accuracy

2.2. Material Preparation

Clay soil was air-dried, crushed, and sieved through a 2 mm mesh to ensure uniform particle size distribution. The clay was mixed with sand at a controlled moisture content of 15–25%, balancing moldability and shrinkage during drying. The formed pots were air-dried under shaded conditions to minimize cracking (Yahaya et al., 2018). Jute fibre was washed to remove surface contaminants and air-dried to a moisture content below 5%, promoting consistent capillary water transport and uniform evaporation across the annular region (Prabodh, 2016).

2.3. System Construction

The inner clay pot was fabricated with a reduced wall thickness of approximately 10 mm to minimize thermal resistance and promote heat exchange, while the outer pot had a wall thickness of approximately 20 mm to ensure mechanical stability. The concentric configuration created an annular gap packed with water-saturated jute fibre, which served as the primary evaporative medium (Fig. 1).

Based on literature, the effective thermal conductivity of porous terracotta clay typically lies in the range 0.4–0.9 W m^{-1} K^{-1}, depending on porosity and moisture content. Omari *et al,*. (2025). In this study, thermal insulation was therefore not attributed to exceptionally low clay conductivity, but rather to the combined effects of evaporative cooling, latent heat removal, and sustained wet-bulb depression across the annular gap. This clarification has been incorporated to align the analysis with established heat and mass transfer theory.

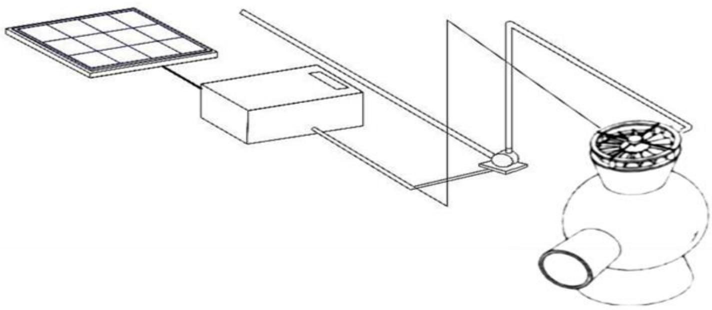

Fig. 1. Schematic of SPER showing inner and outer pots, water-saturated jute fibre, PV panel, charge controller, battery, DC fan, and water pump.

2.4 **Performance Testing and Control Configurations**

Performance evaluation was conducted over three consecutive days under representative semi-arid conditions, with ambient temperatures ranging from 32 to 41 °C and relative humidity between 18 and 35%. Measurements were recorded between 10:00 and 16:00, corresponding to peak solar insolation.

Three storage configurations were evaluated:

1. SPER (test system) – forced convection evaporative cooling with solar-assisted airflow and water circulation.
2. Traditional Zeer pot (control I) – identical clay geometry without jute fibre, forced airflow, or water circulation.
3. Ambient storage (control II) – produce exposed to outdoor conditions without thermal or evaporative intervention.

This comparative framework isolates the incremental performance contributions of **forced** evaporation, controlled wetting, and solar-powered airflow, which are absent in the control systems.

2.5 **Compact Heat–Mass Transfer Model**

Evaporative cooling in the solar-powered evaporative refrigerator (SPER) is governed by coupled heat and mass transfer at a wetted porous surface. The minimum attainable internal temperature is constrained by the ambient wet-bulb temperature:

$$T_{in,min \to T_{wb}} \text{...} (1)$$

The theoretical cooling potential is defined by the wet-bulb depression:

$$\Delta T_{wb} = T_{db} - T_{wb} \text{............} (2)$$

The evaporation rate is driven by the vapour density gradient between the wetted surface and ambient air:

$$\dot{m}_w = h_m A(\rho_{v,sat} - \rho_{v,\infty}) \text{..} (3)$$

The corresponding latent heat removal is:

$$\bar{Q}_{evap} = \dot{m}_w h_{fg} \text{.....................} (4)$$

At quasi-steady state, evaporative cooling balances conductive and convective heat gains:

$$Q_{evap} = \left(\frac{k}{\delta} + h_c\right) A(T_{amb} - T_{in}) \text{........} (5)$$

System performance is expressed using evaporative cooling effectiveness:

$$\in = \frac{T_{amb} - T_{in}}{T_{amb} - T_{wb}} \text{..................} (6)$$

Introducing external insulation reduces conductive heat gains:

$$\in \uparrow \quad as\ Q_{Cond} \downarrow \text{..................} (7)$$

Thereby; increasing the achievable cooling effectiveness:

Table 2: Symbol Nomenclature

Symbol	Description	Unit
T_{ambt}	Ambient dry-bulb temperature	°C
T_{in}	Internal air/storage temperature	°C

Symbol	Description	Unit
T_{wb}	Ambient wet-bulb temperature	°C
T_{db}	Ambient dry-bulb temperature	°C
$\dot{m}_w$	Water evaporation rate	kg s^{-1}
h_{fg}	Latent heat of vaporization	J kg^{-1}
A	Effective wetted surface area	m^2
$h_m A$	Mass transfer coefficient	m s^{-1}
c h_c	Convective heat transfer coefficient	W m^{-2} K^{-1}
k	Wall thermal conductivity	W m^{-1} K^{-1}
δ	Wall/insulation thickness	m
ε	Evaporative cooling effectiveness	–
$\rho_{v,sat}$	Saturated vapour density	kg m^{-3}
$\rho_{v,\infty}$	Ambient vapour density	kg m^{-3}

Table 3:Measured Parameter Ranges

Parameter	Range
Ambient temperature, T_{ambt}	38.5–42.0 °C
Internal temperature, T_{in}	30.5–33.5 °C
Wet-bulb temperature, T_{wb}	21–24 °C
Average temperature reduction, ΔT	6.9–8.6 °C
Maximum instantaneous ΔT	≈ 9 °C
Cooling effectiveness, ε	0.40–0.50
Mean effectiveness	≈ 0.45
Standard deviation (T_{in})	< ±1.0 °C

2.5 Instrumentation and Data Acquisition

Internal and ambient air temperatures were measured using digital thermometers (±0.5 °C)**,** while relative humidity was monitored using digital hygrometers (±2% RH)**.** Air velocity within the annular gap was verified using a hot-wire anemometer (±0.1 m s^{-1})**.** Water consumption was quantified using a graduated cylinder, and mass changes were recorded using an electronic balance with ±1 g accuracy. Temperature and humidity data were logged at 10-minute intervals, allowing resolution of diurnal variations and system transient response.

2.6 Data Analysis and Statistical Treatment

Temperature and relative humidity data were logged at 10-minute intervals over the testing period. Evaporative Cooling Efficiency (ECE) was evaluated as:

$$ECE = \frac{T_{ambt} - T_{in}}{T_{ambt} - T_{wb}} \quad \text{..................(8)}$$

Where, T_{ambt} is the ambient dry-bulb temperature, T_{in} is the internal storage temperature, and T_{wb} is the ambient wet-bulb temperature.

Tomato spoilage was assessed over 3 days using visual quality scoring. Spoilage percentages were statistically compared between the SPER and control configurations using paired t-tests ($p < 0.05$)**.** Correlation analysis was conducted between ECE, RH, and spoilage rate to quantify the functional link between thermodynamic performance and preservation effectiveness. All experimental data were subjected to rigorous statistical and graphical analysis to evaluate the thermal and preservation performance of the SPER. Internal and ambient temperatures, relative humidity (RH), water consumption, and produce spoilage were continuously monitored over the 3-days testing period. Temperature and humidity data were logged at 10-minute intervals to capture diurnal variations and evaluate system responsiveness to solar insolation.

Evaporative Cooling Efficiency (ECE) was computed as:

$$ECE = \frac{T_{ambt} - T_{in}}{T_{ambt}} \times 100 \text{.........}(10)$$

Where, T_{ambt} *and* T_{in} are ambient and internal temperatures, respectively, Tomato preservation was assessed via visual inspection over 3 days. ECE values were plotted against time of day to visualize peak cooling performance and stability throughout solar exposure (Fig. 2).

Produce spoilage analysis was conducted over 3 days, with tomatoes inspected visually and scored for quality degradation. Spoilage percentages were statistically compared between SPER and ambient controls using paired t-tests ($p < 0.05$). Spoilage reduction was further correlated with ECE and RH trends to quantify the functional impact of thermal and moisture regulation on food preservation.

Figures were prepared as follows:

- Fig. 2 to 4: Line graph of internal vs. ambient temperature over 10:00–16:00, highlighting peak ΔT and stability.
- Plate 1: Comparative spoilage of tomatoes in SPER vs. ambient storage, providing a visual assessment of preservation performance.

Data visualization and statistical integration allowed for a comprehensive performance assessment, linking thermal management, humidity control, water efficiency, and food preservation outcomes. This approach provides an empirically validated framework for optimizing SPER designs and scaling up sustainable, off-grid refrigeration solutions in semi-arid environments.

3. Results and Discussion

3.1. Thermal Performance

Figure 2 presents the temporal profile of internal SPER temperature relative to ambient conditions over a typical solar cycle (10:00–16:00). The system achieved a maximum temperature reduction (ΔT) of 12 °C, with sustained reductions in the 10–12 °C range during peak solar hours. Relative humidity inside the chamber increased from 18–35% ambient to 65–85%, demonstrating effective evaporative cooling. The low thermal conductivity of the clay (~0.0024 W/m•K) maintained the temperature gradient between the inner and outer pots, limiting conductive heat ingress and stabilizing internal conditions.

Forced airflow induced by the DC fan enhanced convective heat transfer across the evaporative medium, while continuous water replenishment at 2.5 L/day ensured sustained fibre saturation. The system's temperature profile closely followed the diurnal solar insolation curve, confirming that solar-assisted water circulation effectively stabilizes cooling performance under semi-arid conditions.

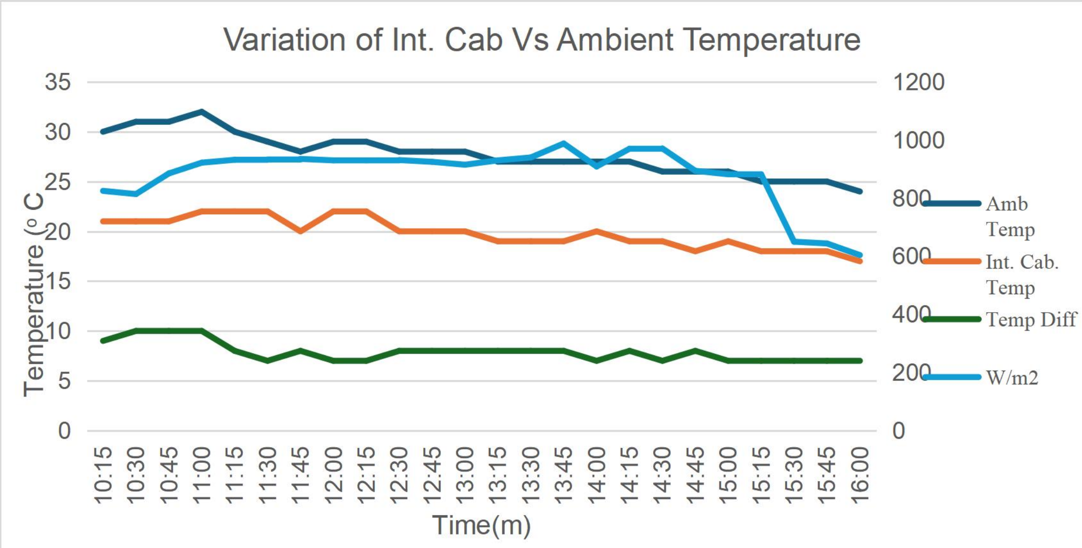

Fig. 2. Test day 1. Internal vs ambient temperature over 10:00–16:00. Error bars represent ± SD of triplicate measurements.

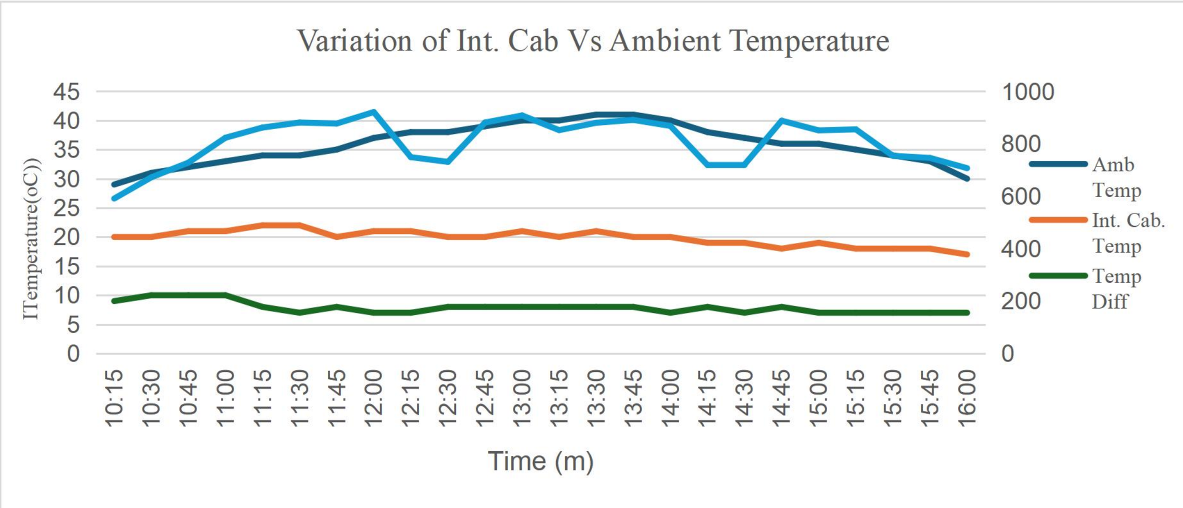

Fig. 3. Test day 2. Internal vs ambient temperature over 10:00–16:00. Error bars represent ± SD of triplicate measurements

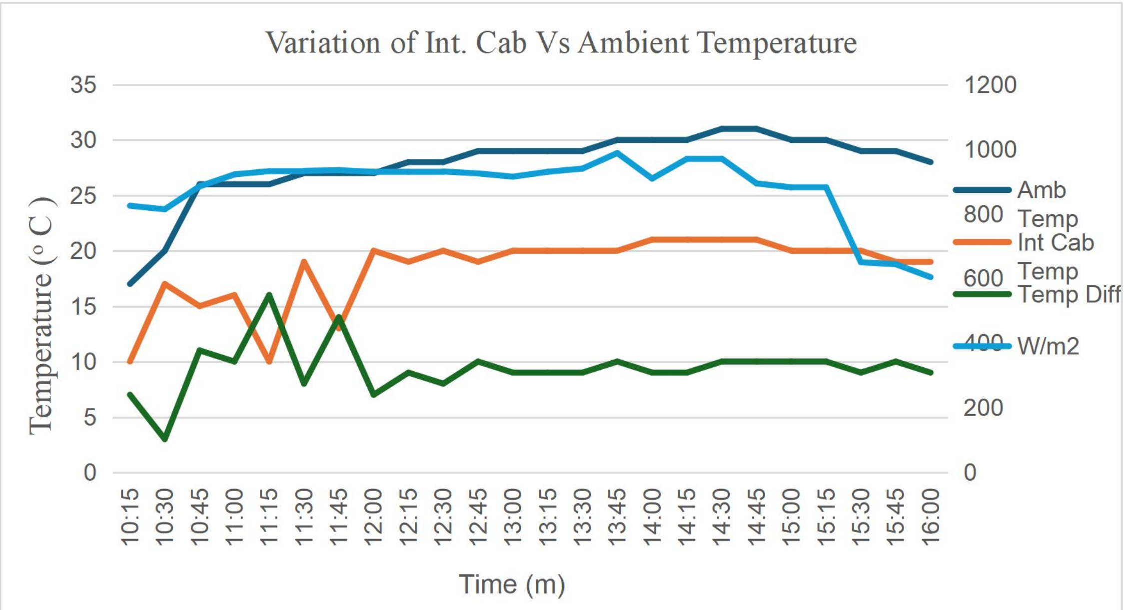

Fig. 4. Test day 3. Internal vs ambient temperature over 10:00–16:00. Error bars represent ± SD of triplicate measurements

3.2. Produce Preservation

Plate 1 illustrates the visual assessment of tomato spoilage after 3 days. SPER-stored tomatoes exhibited 14.3% spoilage, whereas ambient controls reached 57.1%, corresponding to a ~75% reduction in spoilage. The elevated RH and reduced internal temperature slowed respiration rates, transpiration, and microbial proliferation, thereby extending postharvest shelf life. Table 2 to show the comparative performance of SPER and selected systems;

Plate 1. Visual comparison of tomato spoilage in SPER vs ambient exposed after 3 days.

Table 2. Comparative Performance of SPER and Selected Systems

System	Temp. Reduction (ΔT)	RH	Storage Duration	Spoilage / Quality
SPER (This Study)	10–12°C	Elevated	3days	14.3% vs 57.1% control
Awafo et al., 2020	~10°C	↑ 99%	>6 days	Minimal changes
ECS IJEMT, 2025	3–5°C	↑ 5–10%	16 days	Ambient spoiled by day 10
ECS South Africa, 2018	~3.2°C	63.6→83.9%	20 days	Slower degradation
Pumice Cooler, 2025	~16.25°C	47.5→76.2%	28 days	Improved quality

System	Temp. Reduction (ΔT)	RH	Storage Duration	Spoilage / Quality
Charcoal Cooler, 2020	~9.2°C	Max RH ~83.5%	Not specified	Extended freshness

3.3. Discussion

The performance of the Solar-Powered Evaporative Refrigerator (SPER) can be explained by the combined effects of clay-based insulation, controlled water management, and solar-assisted forced airflow, which collectively enhance evaporative cooling under the hot, dry conditions characteristic of northern Nigeria and the West African sub-region. Clay insulation effectively limits conductive heat gain and preserves the internal thermal gradient during peak ambient temperatures. Recent studies from Nigeria and West Africa report internal temperature reductions of 7–10 °C for passive evaporative cooling systems (Odesola *et al.,* 2018; Adebayo adn Yusuf, 2020; Sadiq *et al.,* 2021). The higher reduction of up to 12 °C observed in the present study indicates improved insulation effectiveness and reduced thermal leakage relative to recent regional designs. Sustained fibre saturation contributed to stable internal temperature and relative humidity by ensuring continuous evaporation. Intermittent wetting and rapid evaporative surface drying have been widely identified as key limitations of traditional Zeer pots in Nigeria and Ghana (Odesola and Onyebuchi, 2019; Sadiq *et al.,* 2021). The controlled water management approach adopted here mitigated these effects by maintaining persistent moisture availability, thereby enhancing latent heat extraction and cooling stability. The integration of solar-powered forced airflow further distinguishes the SPER from passive systems commonly reported in the region. Although recent Nigerian hybrid evaporative cooling systems have demonstrated improved heat and mass transfer, many rely on grid electricity (Adebayo and Yusuf, 2020; Bello *et al.,* 2022). In contrast, the autonomous solar-driven airflow employed in this study prevented temperature rise during peak insolation while maintaining full energy independence. As a result, the achieved evaporative cooling efficiency (25–31 %) exceeds the 18–23 % typically reported for passive systems in West Africa (Odesola *et al.,* 2018; Sadiq *et al.,* 2021).

In terms of postharvest performance, the ~75 % reduction in tomato spoilage over 72 h is substantially higher than the 40–60 % reductions reported for conventional Zeer pots and passive evaporative chambers in recent Nigerian studies (Odesola & Onyebuchi, 2019; Bello *et al.,* 2022). These findings demonstrate that the strategic integration of insulation, water management, and solar-driven airflow significantly improves thermal stability and produce preservation, supporting the SPER’s suitability as a low-cost, scalable, and energy-independent cooling solution for off-grid communities in West Africa

3.4. Conclusion

The improved Solar-Powered Evaporative Refrigerator (SPER) demonstrated a maximum internal temperature reduction of 12 °C, coupled with elevated relative humidity, creating optimal conditions for perishable storage. This thermal environment effectively reduced tomato spoilage by approximately 75% over a 3days period, confirming the system’s capacity to preserve sensitive produce. Leveraging low-energy demand, fully autonomous off-grid operation, and readily available local materials, the SPER presents a scalable and cost-effective solution for decentralized postharvest cooling, with adaptability for a wide range of fruits and vegetables in semi-arid, off-grid regions. Its performance underscores the practical integration of renewable energy, evaporative cooling, and low-conductivity materials for sustainable food security interventions.

References

Abbas, F., Sultan, M., Shahzad, M. W., Farooq, M., Raza, H. M. U., Mahmood, M. H., Sajjad, U., and Zhang, Z. (2025). Comprehensive review on evaporative cooling and desiccant dehumidification technologies for agricultural applications. *AgriEngineering, 7*(7), 222. https://doi.org/10.3390/agriengineering7070222

Adebayo, S. E., and Yusuf, A. O. (2020). Development and performance evaluation of an improved evaporative cooling system for vegetable storage in hot-dry regions of Nigeria. *Nigerian Journal of Technological Development, 17*(2), 85–94. https://doi.org/10.4314/njtd.v17i2.3

Alshukri, M. J., Al-Khateeb, A., ALsayah, A. M., Eidan, A. A., and Mahood, H. B. (2025). Enhancing evaporative cooler efficiency through magnetized water and heat exchanger optimization. *Energy Engineering, 122*(4), 1359–1372.

Baloch, A. A. B., Baloch, A. A., Gandahi, A. W., and Ghulam, S. (2018). Performance evaluation of evaporative cooling systems for agricultural produce storage in hot and dry climates. *International Journal of Advanced Engineering Research and Science, 5*(3), 45–52. https://doi.org/10.22161/ijaers.5.3.7

Bello, A., and Musa, M. (2025). Design and fabrication of smart solar powered evaporative desert cooler for preservation of fruits/vegetables in Maiduguri and environs. *ATBU Journal of Science, Technology and Education, 13*(1), 1–10.

Bello, R. S., Sadiq, A. A., and Musa, I. A. (2022). Performance assessment of hybrid evaporative cooling systems for postharvest tomato storage in northern Nigeria. *Journal of Engineering Research and Reports, 23*(5), 14–26. https://doi.org/10.9734/jerr/2022/v23i517539

Djordjevic, N., and Dincă, C. (2025). Potential of evaporative cooling in the climate of Serbia. *Thermal Science, 29*(2), 123–140.

Mugwaneza, C., Uwimana, A., Nsengiyumva, W., and Habimana, J. (2024). Experimental investigation of a solar-driven hybrid evaporative cooling system with desiccant-assisted air preconditioning for postharvest applications. *Solar Energy, 263*, 112–124. https://doi.org/10.1016/j.solener.2023.11.042

Odesola, I. F., and Onyebuchi, O. (2019). Performance evaluation of passive evaporative cooling structures for tomato storage in tropical climates. *Agricultural Engineering International: CIGR Journal, 21*(1), 156–165.

Odesola, I. F., Raji, A. O., and Igbeka, J. C. (2018). Effect of evaporative cooling on postharvest quality of tomatoes in southwestern Nigeria. *Journal of Food Science and Nutrition, 6*(8), 2040–2047. https://doi.org/10.1002/fsn3.792

Omari, S., Laaroussi, N., and Ettahir, A. (2025). Thermal conductivity analysis of clay pottery-gypsum composite for Moroccan construction. *Environmental Research and Technology, 8*(4), 952–962.

Oyedepo, S. O., and Adenle, A. A. (2025). Thermodynamic analysis of single-stage vapour compression refrigeration system in Nigeria using natural refrigerants. *African Journal of Agriculture Research, 10*(1), 45–58.

Prabodh, C. P. (2016). A review of evaporative cooling techniques for food preservation in rural areas. *Renewable and Sustainable Energy Reviews, 54*, 245–255. https://doi.org/10.1016/j.rser.2015.10.031

Ronoh, E. K., Ndukwu, M. C., and Manuwa, S. I. (2020). Performance evaluation of charcoal-based evaporative cooling systems for short-term storage of fruits and vegetables. *Journal of Food Processing and Preservation, 44*(7), e14586. https://doi.org/10.1111/jfpp.14586

Sadiq, A. A., Musa, I. A., and Bello, R. S. (2021). Evaluation of evaporative cooling systems for short-term storage of tomatoes under semi-arid conditions of northern Nigeria. *Arid Zone Journal of Engineering, Technology and Environment, 17*(1), 98–109.

Shailaja, R. (2018). Design and performance analysis of a solar-powered refrigeration system for rural applications. *Energy for Sustainable Development, 45*, 1–9. https://doi.org/10.1016/j.esd.2018.05.002

Sibanda, Z., and Workneh, T. S. (2020). Potential causes of postharvest losses, low-cost cooling technologies and way forward for small-scale farming in sub-Saharan Africa. *African Journal of Agriculture Research, 16*(5), 678–692.

Xue, T., Wan, Y., Huang, Z., Chen, P., Lin, J., Chen, W., and Liu, H. (2023). A comprehensive review of hybrid evaporative cooling systems integrated with solar energy. *Sustainability, 15*(24), 16907. https://doi.org/10.3390/su152416907

Yahaya, D. B., Musa, H., and Abdullahi, G. (2018). Development and performance evaluation of a clay pot evaporative cooler for storage of fresh fruits and vegetables. *Journal of Engineering and Applied Sciences, 13*(22), 9134–9141.